

# Effect of a bimolecular chemical reaction on the convective dissolution of CO<sub>2</sub>

Sylvain Kabbadj, Laurence Rongy, Anne De Wit, and Andy Woods \*

**Abstract** Upon dissolution of a phase A into another one below it, a density stratification arises with a denser fluid above a less dense one if A increases the density of the solution. This gives rise to convective dynamics. The convective dissolution of A can be influenced by a chemical reaction because the reaction impacts the density profile. We theoretically focus on the reaction between species A and B initially present in the host phase producing C through the bimolecular  $A + B \rightarrow C$  reaction. We numerically analyse the influence of the chemical reaction on the convective dynamics in the host phase and on the dissolving flux of A through the interface, depending on whether the reaction stabilizes or destabilizes the density profile. We show that the rate of advancement of the reaction front in the stabilizing case is controlled by both the diffusion of the reactants and by the convection of A above the reaction zone. With these results, we improve our understanding on the optimization of CO<sub>2</sub> (A) sequestration into an aquifer containing a reactant (B).

---

Sylvain Kabbadj  
Université libre de Bruxelles, Belgium  
e-mail: sylvain.kabbadj@ulb.be

Laurence Rongy  
Université libre de Bruxelles, Belgium

Anne De Wit  
Université libre de Bruxelles, Belgium

Andy Woods  
University of Cambridge, United Kingdom

\* This report presents the results of a project undertaken by the first author at the Matrix Workshop *Instabilities in Porous Media*, April 3-23, 2024, under the supervision of the other authors.

## 1 Introduction

Upon dissolution of carbon dioxide ( $\text{CO}_2$ ) in an aqueous solution in the context of its geological sequestration,  $\text{CO}_2$  increases locally the density of the host phase leading to a stratification of a denser phase above a less dense one. This so-called buoyantly unstable density gradient can lead to convective dynamics [2, 3, 4, 5, 11] that can be influenced by reactions [6, 7].

In this work, we study theoretically a reactive system in which species A ( $\text{CO}_2$ ) dissolves into a host phase where it reacts with species B to produce C via the simple  $A + B \rightarrow C$  reaction. It has been shown that the reaction modifies the solute concentrations, which affects the density profile and the dynamics in the host phase [1, 6, 7, 9, 10]. In particular, the reaction consuming A can slow down or accelerate the development of the convection compared to the nonreactive case, leading to stabilizing or destabilizing cases, respectively [6, 8, 10].

Our goal is to extend our understanding of the stabilizing effect of the reaction on the convective dynamics. In this stabilizing case, it is known that the convection is stuck behind a reaction front. We aim to determine what is the rate of advancement of the reaction front in the host phase and how it is controlled. Furthermore, we aim to use these new results to understand whether there is a limit to the destabilization of the system and how it is controlled.

## 2 Model

We study a partially miscible system containing a phase of pure A above a host phase containing a solvent and a reactant B. Upon dissolution of A into the host phase, the bimolecular  $A + B \rightarrow C$  reaction produces the product C with a reaction rate defined as  $q\tilde{A}\tilde{B}$  where  $q$  is the kinetic constant and  $\tilde{A}$  and  $\tilde{B}$  are the concentrations of A and B respectively. The gravity field points downwards along the  $\tilde{z}$  axis and perpendicular to the  $\tilde{x}$  axis as represented in Fig. 1. We consider that the system is isothermal, isotropic and homogeneous, that the diffusion coefficients are constant, that no mass transfer takes place between the host phase and the upper phase of pure A and that the solubility of A in the host phase is a constant. The horizontal length of the system extends from  $\tilde{x} = 0$  to  $\tilde{x} = \tilde{L}_x$  and its height goes from  $\tilde{z} = 0$  to  $\tilde{z} = \tilde{L}_z$ .

We non-dimensionalize the variables using:

$$t = \frac{\tilde{t}}{t_c}, \quad x = \frac{\tilde{x}}{l_c}, \quad z = \frac{\tilde{z}}{l_c}, \quad \mathbf{u} = \frac{\tilde{\mathbf{u}}}{u_c}, \quad (1a)$$

$$A = \frac{\tilde{A}}{A_0}, \quad B = \frac{\tilde{B}}{A_0}, \quad C = \frac{\tilde{C}}{A_0} \quad (1b)$$

where tildes stand for dimensional variables. The time and length are normalized using the characteristic reaction-diffusion (RD) length scale and chemical time scale [7, 8, 9]  $l_c = \sqrt{D_A t_c}$  where  $D_A$  is the diffusion coefficient of A and  $t_c = 1/(qA_0)$ .

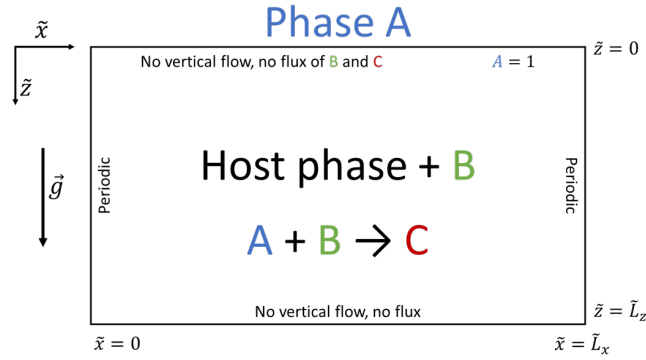


Fig. 1: Schematic of the two-dimensional model used to analyse the reactive convective dissolution of A into the host phase where a reaction between A and B produces C.

$A_0$ , used to normalize the solute concentrations  $A$ ,  $B$  and  $C$ , is the solubility of A in the initial solution of B with concentration  $B_0$ . The velocity field  $\tilde{\mathbf{u}} = (\tilde{u}_x, \tilde{u}_z)$  is normalized by the velocity scale  $u_c = \phi \sqrt{D_A q A_0}$  where  $\phi$  is the porosity of the medium.

Dropping tildes, the dimensionless equations governing the reaction-diffusion-convection (RDC) evolution of the concentrations of A, B and C in the host phase are:

$$\frac{\partial A}{\partial t} + (\mathbf{u} \cdot \nabla)A = \nabla^2 A - AB, \quad (2a)$$

$$\frac{\partial B}{\partial t} + (\mathbf{u} \cdot \nabla)B = \delta_B \nabla^2 B - AB, \quad (2b)$$

$$\frac{\partial C}{\partial t} + (\mathbf{u} \cdot \nabla)C = \delta_C \nabla^2 C + AB \quad (2c)$$

where  $\delta_I = D_I/D_A$  is the diffusion coefficient of species I normalized by the one of species A. We solve Eqs. (2) with the initial conditions:

$$A(x, z = 0, t = 0) = 1 + \varepsilon \text{rand}(x); \quad A(x, z > 0, t = 0) = 0, \quad (3a)$$

$$B(x, z, t = 0) = \beta, \quad (3b)$$

$$C(x, z, t = 0) = 0 \quad (3c)$$

where  $\beta = B_0/A_0$  is the initial concentration of B normalized by the solubility of A in the initial solution of B and  $\varepsilon \text{rand}(x)$  is a perturbation introduced at the interface to trigger the instability.  $\varepsilon = 10^{-3}$  is the amplitude of the perturbation and  $\text{rand}(x)$  is a random noise along the  $x$  axis between  $-1$  and  $1$ . Normalizing the length and height of the system using the notations  $L_z = \tilde{L}_z/l_c$  and  $L_x = \tilde{L}_x/l_c$ , the boundary conditions are taken as:

$$u_z(z=0) = 0; \quad u_z(z=L_z) = 0; \quad \mathbf{u}(x=0) = \mathbf{u}(x=L_x), \quad (4a)$$

$$A(z=0, t > 0) = 1; \quad \left. \frac{\partial A}{\partial z} \right|_{z=L_z} = 0; \quad A(x=0) = A(x=L_x), \quad (4b)$$

$$\left. \frac{\partial B}{\partial z} \right|_{z=0} = 0; \quad \left. \frac{\partial B}{\partial z} \right|_{z=L_z} = 0; \quad B(x=0) = B(x=L_x), \quad (4c)$$

$$\left. \frac{\partial C}{\partial z} \right|_{z=0} = 0; \quad \left. \frac{\partial C}{\partial z} \right|_{z=L_z} = 0; \quad C(x=0) = C(x=L_x). \quad (4d)$$

Darcy's law in porous media is used to compute the fluid flow velocity while Poisson's equation is used to express the flow incompressibility condition. These equations read:

$$\nabla p = -\mathbf{u} + \rho \mathbf{e}_z, \quad (5a)$$

$$\nabla^2 p = \nabla \cdot (\rho \mathbf{e}_z) \quad (5b)$$

where  $p$  is the pressure.

We consider that the density change is the driving force of the convective dynamics and assume a linear state equation for the density as a function of the concentrations:

$$\tilde{\rho} = \rho_0 (1 + \alpha_A \tilde{A} + \alpha_B \tilde{B} + \alpha_C \tilde{C}) \quad (6)$$

where  $\rho_0$  is the density of the pure solvent and  $\alpha_I = \frac{1}{\rho_0} \frac{\partial \tilde{\rho}}{\partial \tilde{c}_I}$  is the solutal expansion coefficient of species I. A dimensionless density is computed as:

$$\frac{\tilde{\rho} - \rho_0}{\rho_c} = R_A A + R_B B + R_C C \quad (7)$$

where  $\rho_c = \phi \mu D_I / (g \kappa l_c)$  is the density scale,  $\kappa$  is the permeability of the porous medium and  $\mu$  is the viscosity of the fluid.  $R_I$  is the Rayleigh number of species I:

$$R_I = \frac{\alpha_I A_0 g \kappa l_c}{\phi \nu D_A} = \frac{\alpha_I A_0 g \kappa}{\phi \nu \sqrt{D_A} q A_0} \quad (8)$$

where  $\nu = \mu / \rho_0$  is the kinematic viscosity of the solvent.

We consider that all species diffuse at the same rate, *i.e.*  $\delta_B = \delta_C = 1$ . Summing Eqs. (2b) and (2c) evidences that we have then the conservation relation:  $B + C = \beta$  [7, 10]. We then define the dimensionless density  $\rho$  as:

$$\rho = \frac{\tilde{\rho} - \rho_0}{\rho_c} - R_B \beta = R_A A + \Delta R_{CB} C \quad (9)$$

where  $\Delta R_{CB} = R_C - R_B$ . To summarize, the dimensionless parameters controlling the dynamics are the initial concentration of B ( $\beta = 0$  in the nonreactive case and  $\beta = 1$  in reactive cases), the Rayleigh number of A ( $R_A = 1$  in this work) and  $\Delta R_{CB}$  ( $\Delta R_{CB} = +1$  in the destabilizing case and  $\Delta R_{CB} = -1$  in the stabilizing case).

### 3 Nonlinear simulations

We numerically solve the model with  $L_x = 3072$  and  $L_z = 2048$  on COMSOL Multiphysics version 6.0. We compute the density field and calculate the flux of A entering the host phase through the interface ( $z = 0$ ) in three cases: the nonreactive (NR) case where the initial concentration of B is zero ( $\beta = 0$ ) and two reactive cases ( $\beta = 1$ ). We first compare our results at early times with the literature [6, 10] then we analyse them at late times to extend our understanding of the stabilizing and destabilizing effects of the reaction on the density field and on the flux of A.

#### 3.1 Nonreactive case (NR)

Upon dissolution of A into the host phase in the absence of reaction, the density field  $\rho$  given by Eq. (9) equals A as  $R_A = 1$  and there is no C produced. The temporal evolution of the density is shown in Fig. 2.

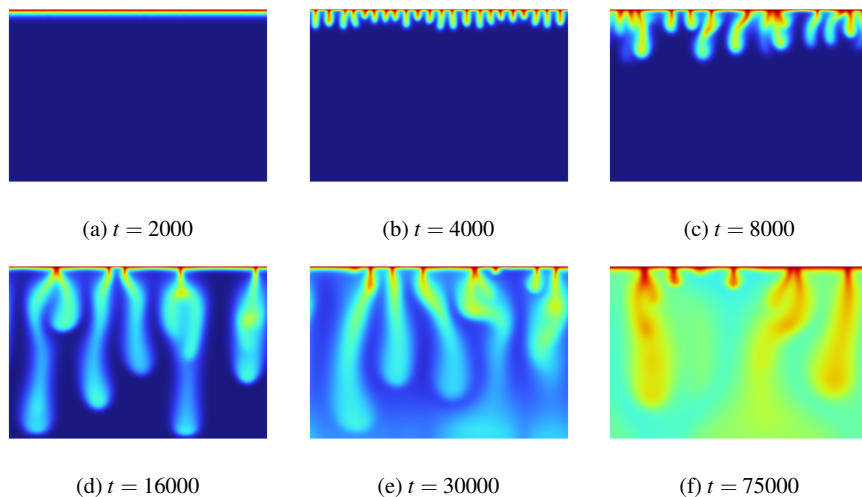


Fig. 2: Temporal evolution of the density field in the host solution in the nonreactive case ( $\beta = 0$ ). The density scale varies from 0 (blue) to 1 (red).

First, A diffuses downwards into the host phase (Fig. 2a). Since  $R_A = 1$ , the upper phase containing dissolved A is denser than the host phase, leading to the onset of buoyancy-driven convection (Fig. 2b). The so-called fingers of the denser fluid sink and interact with each other with a merging that increases over time (Fig. 2c-2d). The fingers of the dense solution then reach the bottom of the host layer and the dynamics enter the so-called shutdown regime (Fig. 2e-2f).

### 3.2 Reactive destabilizing case: $\Delta R_{CB} = +1$

The presence of a reactant in the host phase can destabilize the system, i.e. increase the intensity of convection and accelerate its onset. This occurs when the reaction produces a species C that is sufficiently denser than the reactants, which is the case when ( $\Delta R_{CB} > 0$ ). An example of convective dynamics accelerated by reaction is shown for  $\Delta R_{CB} = +1$  in Fig. 3.

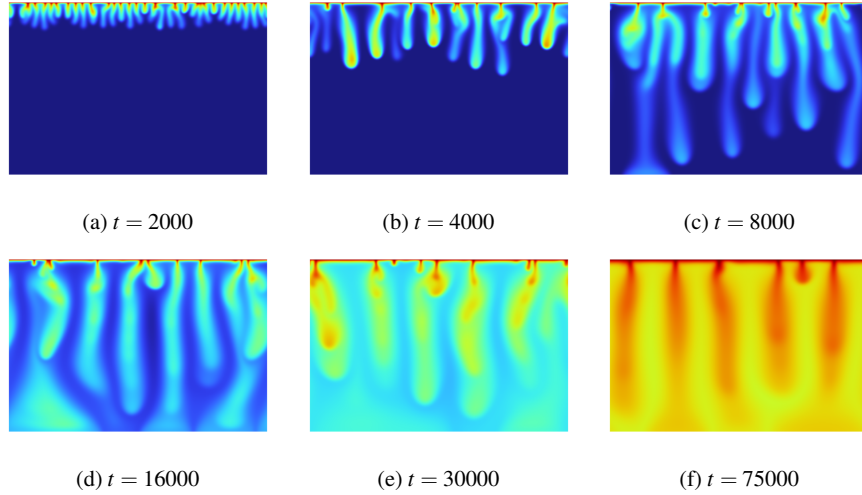


Fig. 3: Temporal evolution of the density field in the host solution in the destabilizing reactive case ( $\beta = 1$  and  $\Delta R_{CB} = +1$ ). The density scale varies from 0 (blue) to 2 (red).

The intensity of the density changes is larger than in the nonreactive case (Fig. 2) and the convection starts earlier. The number of fingers also increases compared to the NR case while the shutdown of the system is reached already at  $t = 8000$ . At later times, merging decreases and descending fingers start to only be visible vertically, separated by a fixed distance.

We quantify the destabilizing effect of the reaction on the flux by computing the dissolving flux of A through the interface as:

$$J_{RDC} = -\frac{1}{L_x} \int_0^{L_x} \left. \frac{\partial A}{\partial z} \right|_{z=0} dx. \quad (10)$$

Figure 4 compares the temporal evolution of the flux in the reactive case (reaction-diffusion-convection), in absence of convection (reaction-diffusion), in absence of reaction (diffusion-convection, corresponding to the NR case presented in Sect. 3.1) and in absence of both reaction and convection (diffusion).

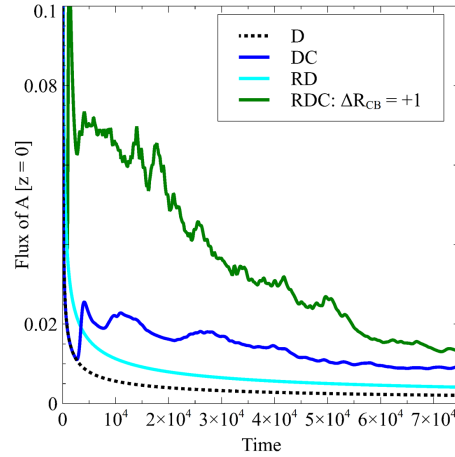


Fig. 4: Temporal evolution of the flux of A through the interface ( $z = 0$ ) in the destabilizing reactive case ( $\beta = 1$  and  $\Delta R_{CB} = +1$ ) compared to cases controlled only by diffusion (D), diffusion-convection (DC) and reaction-diffusion (RD).

The dissolving flux of A increases due to the reaction (RD) and due to the convection (DC) compared to the diffusive case (D). Most importantly, the reaction is known to modify the density profile which itself modifies the convective dynamics. In the destabilizing case, the combined effects of the reaction and of convection (RDC) greatly increase the flux compared to all other cases. We note that the early start of convection compared to the DC case is observed by an earlier increase in the flow, the latter leaving its diffusive profile when the convective dynamics rise. The flow oscillations are then due to the merging phenomenon of the fingers. Finally, the RDC flux decreases over time because of the shutdown of the dynamics [12].

### 3.3 Reactive stabilizing case: $\Delta R_{CB} = -1$

Figure 5 shows the temporal evolution of the density change in the host phase if the reaction stabilizes convection by consuming A and producing a product C less dense than the reactants ( $\Delta R_{CB} < 0$ ).

First, we note that convection starts later than in previously described cases, i.e. the diffusive regime lasts longer (Fig. 5a-5b). Moreover, the reaction decreases the density locally, creating a minimum in the density profile at the reaction front. We observe convection above this minimum, i.e. above the reaction front, where the denser phase is located above a less dense phase. The convective dynamics remain confined above the reaction front because the host phase below it is denser. Merging is less frequent than in the destabilizing case (Fig. 5c-5e) and is not observed at later times, where the fingers tend to develop only vertically (Fig. 5f).

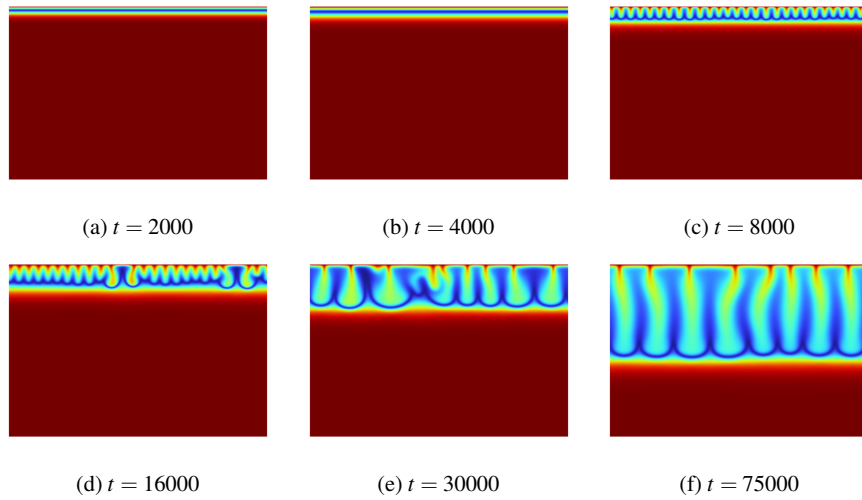


Fig. 5: Temporal evolution of the density field in the host solution in the stabilizing reactive case ( $\beta = 1$  and  $\Delta R_{CB} = -1$ ). The density scale varies from  $-1$  (blue) to  $0$  (red).

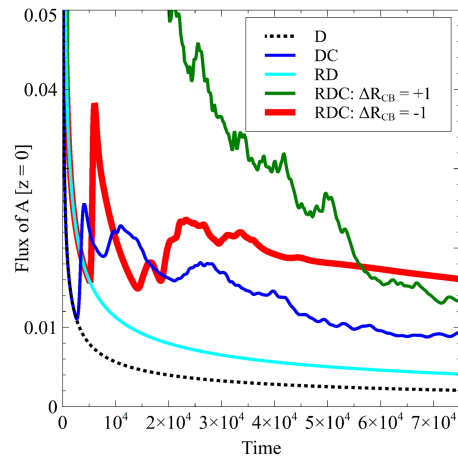


Fig. 6: Temporal evolution of the flux of  $A$  through the interface ( $z = 0$ ) in the stabilizing reactive case ( $\beta = 1$  and  $\Delta R_{CB} = -1$ ) compared to cases controlled only by diffusion ( $D$ ), diffusion-convection ( $DC$ ) and reaction-diffusion ( $RD$ ).

Figure 6 shows the flux of A in the stabilizing case compared to the previously studied cases. The combined effects of the reaction and of convection increase the flux compared to its RD and DC counterparts. However, the flux is smaller than in the destabilizing case because A is carried less far into the host phase, so its concentration gradient is smaller. After a long time, i.e.  $t \approx 45000$ , the flux decreases linearly over time. This phenomenon is due to the absence of merging and the almost exclusively vertical growth of the fingers. Note that the flux then becomes larger than its destabilizing counterpart because of the shutdown of the system that is not yet observed in the stabilizing case.

Finally, we calculate the rate of advancement of the reaction front into the host phase. We horizontally average the density profiles to get  $\langle \rho(z, t) \rangle$  and calculate the mixing length as the distance between the interface and the vertical position beyond which  $\langle \rho(z, t) \rangle > -0.01$ . The temporal evolution of the mixing length is presented in Fig. 7.

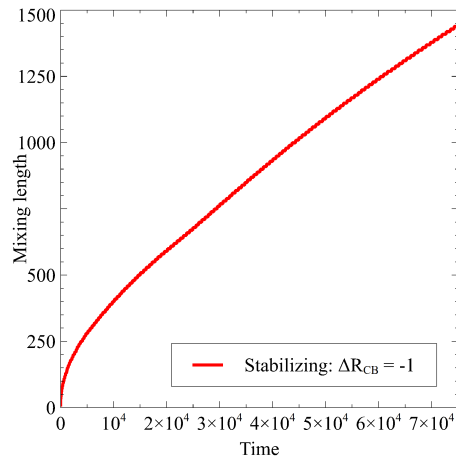


Fig. 7: Temporal evolution of the mixing length (the vertical extent of the zone in which convective dynamics are confined) in the stabilizing reactive case ( $\beta = 1$  and  $\Delta R_{CB} = -1$ ).

In the diffusive regime, the reaction front advances according to a  $t^{1/2}$  scaling. Once the convective dynamics start, the reaction front invades the host phase faster. The position of the narrow region in which the reaction occurs depends on the supply of B which is only controlled by its upward diffusion and the supply of A which is controlled both by its downward diffusion and by its convection. Since the convective dynamics are confined behind the reaction front, A is the only reactant that is advected to the reaction zone. Finally, we note that the rate of advancement of the front is also controlled by  $\beta$ . Indeed, if the host phase is initially more concentrated in B, the supply of this reactant to the reaction front is higher and the advancement of the front is slower.

The differences between the nonreactive, destabilizing and stabilizing cases are summarized in Fig. 8 as space-time plots of the density.

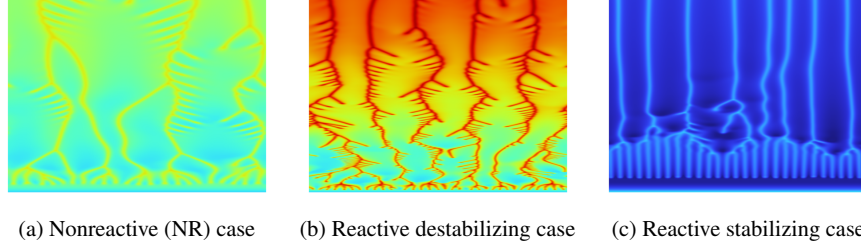


Fig. 8: Space-time plots of the density at  $z = 64$  for the nonreactive case ( $\beta = 0$ ) and the reactive destabilizing ( $\beta = 1$  and  $\Delta R_{CB} = +1$ ) and stabilizing ( $\beta = 1$  and  $\Delta R_{CB} = -1$ ) cases. The density scale varies from  $-1$  (blue) to  $2$  (red). The vertical axis is time, going upwards from  $t = 0$  to  $t = 75000$ .

The different regimes are observed by analysing the temporal evolution of the density along one line ( $z = 64$ ) situated below the interface. We observe that the convection starts first in the destabilizing case, later in the nonreactive case and even later in the stabilizing case. At early times, merging is observed in all cases and is more important in the destabilizing case than in the NR case, in which it is more important than in the stabilizing case. Furthermore, we note that the amplitude of the density change also follows the same trend. The reaction increases the initial number of fingers in both reactive cases compared to the NR case. Finally, we also observe in the stabilizing case that the merging between the fingers stops early and that the fingers then grow vertically without interacting with each other.

To understand if fingers grow infinitely without interacting with each other in the stabilizing case, we analysed the horizontally averaged density profiles and the flux of A at later times, as presented in Fig. 9.

We observe two minima in the averaged density profiles (Fig. 9a): one located at the reaction front due to the production of C which decreases locally the density and one that develops near the interface where a new merging regime is observed. The first minimum located at the reaction front explains the confinement of the convective dynamics behind this front because the fluid is locally less dense than the fluid below. The second minimum located near the interface shows that a new merging phenomenon rises at late times. This new regime is also observed in the flux of A (Fig. 9b); after a long linear decrease of the flux due to the vertical growth of the fingers, the flux increases and oscillates again.

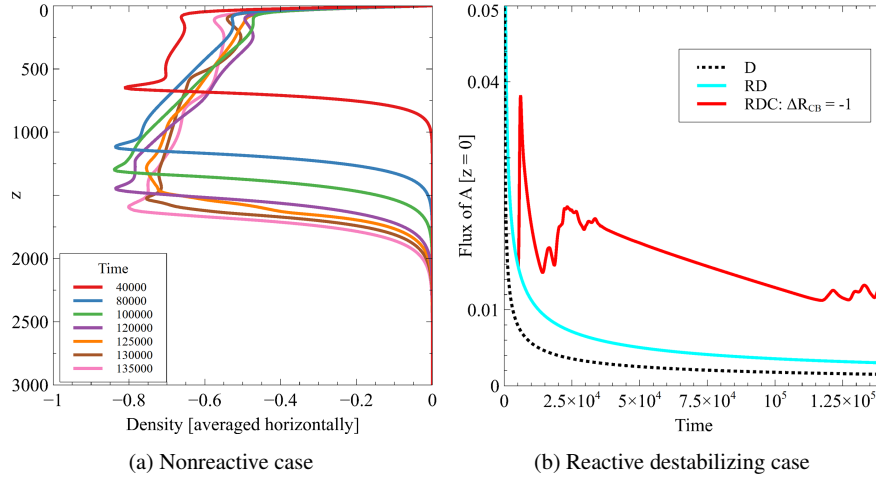


Fig. 9: Later time evolution in the stabilizing reactive case ( $\beta = 1$  and  $\Delta R_{CB} = -1$ ): (a) horizontally averaged density profiles as a function of  $z$  and (b) flux of A through the interface ( $z = 0$ ).

## 4 Conclusions

Upon dissolution of A into a host phase containing a reactant B, the bimolecular  $A + B \rightarrow C$  reaction producing C can stabilize the system if the product decreases the density of the fluid ( $\Delta R_{CB} = -1$ ). In this case, the reaction produces a local minimum in the density profile, leading to the confinement of the convective dynamics above the reaction front. We studied numerically the rate of advancement of the reaction front which is controlled by the supply of B (upwards diffusion of B) and by the supply of A (downwards diffusion of A and convection transporting A) to the reaction zone. We quantified the influence of the combined effects of the reaction and the convective dynamics on the dissolving flux of A through the interface in both the destabilizing and stabilizing reactive cases focusing in particular on later times close to the shutdown regime.

This study opens perspectives for future works. First, we could analyse the influence of an initially stratified concentration of B or an initial gradient in its concentration, which could help understand the influence of  $\beta$  on the rate of advancement of the front. The stabilizing case could be studied at later times ( $t \approx 500000$ ) to observe the rise of multiple merging regimes. The understanding of the factors controlling the merging of the fingers in the stabilizing case could help understand what controls the shutdown of the system in the destabilizing case. Overall, these results could lead to a better understanding of the chemical control of the shutdown of convective systems at high Rayleigh number.

## References

1. Cardoso S. and Andres J.: Geochemistry of silicate-rich rocks can curtail spreading of carbon dioxide in subsurface aquifers. *Nat. Commun.* **5**, 5743 (2014).
2. De Paoli M.: Convective mixing in porous media: a review of Darcy, pore-scale and Hele-Shaw studies. *Eur. Phys. J. E* **46**, 129 (2023).
3. Emami-Meybodi H., Hassanzadeh H., Green C.P. and Ennis-King J.: Convective dissolution of CO<sub>2</sub> in saline aquifers: Progress in modeling and experiments. *Int. J. of Greenhouse Gas Control* **40**, 238–266 (2015).
4. Hewitt D.R.: Vigorous convection in porous media. *Proc. R. Soc. A: Math. Phys. Eng. Sci.* **476**, 20200111 (2020).
5. Huppert H.E. and Neufeld J.A.: The fluid mechanics of carbon dioxide sequestration. *Annu. Rev. Fluid Mech.* **46**, 255–272 (2014).
6. Jotkar M., De Wit A. and Rongy L.: Enhanced convective dissolution due to an A + B → C reaction: control of the non-linear dynamics *via* solutal density contributions. *Phys. Chem. Chem. Phys.* **21**, 6432 (2019).
7. Loodts V., Thomas C., Rongy L. and De Wit A.: Control of convective dissolution by chemical reactions: General classification and application to CO<sub>2</sub> dissolution in reactive aqueous solutions. *Phys. Rev. Lett.* **113**, 114501 (2014).
8. Loodts V., Rongy L. and De Wit A.: Chemical control of dissolution-driven convection in partially miscible systems: Theoretical classification. *Phys. Chem. Chem. Phys.* **17**, 29814–29823 (2015).
9. Loodts V., Trevelyan P.M.J., Rongy L. and De Wit A.: Density profiles around A + B → C reaction-diffusion fronts in partially miscible systems: A general classification. *Phys. Rev. E* **4**, 043115 (2016).
10. Loodts V., Knaepen B., Rongy L. and De Wit A.: Enhanced steady-state dissolution flux in reactive convective dissolution. *Phys. Chem. Chem. Phys.* **19**, 18565–18579 (2017).
11. Neufeld J.A., Hesse M.A., Riaz A., Hallworth M.A., Tchelepi H.A. and Huppert H.E.: Convective dissolution of carbon dioxide in saline aquifers. *Geophys. Res. Lett.* **37**, L22404 (2010).
12. Slim A.C.: Solutal-convection regimes in a two-dimensional porous medium. *J. Fluid Mech.* **741**, 461–491 (2014).